A EUROPEAN JOURNAL OF CHEMICAL BIOLOGY

CHEMBIOCHEM

SYNTHETIC BIOLOGY & BIO-NANOTECHNOLOGY

Accepted Article

Title: Time-Dependent Cytotoxic Properties of Terpyridine-Based Copper Complexes

Authors: Jordi Grau, Amparo Caubet, Olivier Roubeau, David Montpeyó, Julia Lorenzo, and Patrick Gamez

To be cited as: *ChemBioChem* 10.1002/cbic.202000154

Link to VoR: http://dx.doi.org/10.1002/cbic.202000154

A Journal of ChemPubSoc Europe

WILEY-VCH

www.chembiochem.org

Time-Dependent Cytotoxic Properties of Terpyridine-Based Copper Complexes

Jordi Grau,[a] Amparo Caubet,*[a] Olivier Roubeau,[b] David Montpeyó,[c] Julia Lorenzo[c] and Patrick Gamez*[a,d,e]

Abstract: Five copper complexes supported by terpyridine ligands were prepared and characterized, *viz*. $[Cu_3Cl_4(\mathbf{Naphtpy})_2][CuCl_2]$ (**1**), $[Cu_2Cl_2(\mathbf{Naphtpy})_2](ClO_4)_2$ (**2**), $[CuCl_2(\mathbf{Naphtpy})]_2(MeOH)_3(H_2O)$ (**3**), $[CuCl_2(\mathbf{Cltpy})]$ (**4**) and $[Cu(\mathbf{Cltpy})_2](ClO_4)_2$ (**5**); (where **Naphtpy** stands for 4'-((naphthalen-2-yl)methoxy)-2,2′:6′,2″-terpyridine and **Cltpy** for 4′-chloro-2,2′:6′,2″-terpyridine). Their DNA-interaction abilities were investigated, and their cytotoxic behaviors were examined with three cells lines, namely with human ovarian carcinoma cells (A2780) and its derived cisplatin-resistant line (A2780cis), and human cervix adenocarcinoma cells (HeLa). All compounds show good cytotoxic properties (especially after 72 h incubation). Remarkably, two compounds, *i.e.* **4** and **5**, are almost inactive after 24 h (particularly **4**), but are highly active after 72 h, with IC_{50} values in the low micromolar to submicromolar range. Compounds **1** and **2** induce necrosis, whereas late apoptosis is observed with **3**–**5**, **4** exhibiting a behaviour close to that of cisplatin.

Introduction

Nucleases are enzymes capable of cleaving DNA by rapidly hydrolyzing its phosphodiester bond.[1, 2] These biological catalysts are involved in a variety of biological functions, including DNA replication, recombination, repair, regulation, processing and degradation.[2, 3] Over the last three decades, research efforts have been dedicated to the design of small coordination compounds that mimic nuclease activity.[4] Such hydrolytically-cleaving metallonucleases have been used to substitute restriction enzymes or footprinting agents, and as simple models to elucidate the mechanism of action of the natural enzymes.[3, 5]

When the coordination compounds contain redox-active metal ions, the oxidative cleavage of DNA may occur.[6] For example, the binding of iron to the glycopeptide bleomycin generates a complex with anticancer properties,[7] which are attributed to its ability to cleave DNA oxidatively.[8] Hence, a great number of artificial metallonucleases (AMNs) have been described in the literature for their potential use as anticancer agents.[3, 9] From the different transition metals used, copper appears to be one of the most attractive; indeed, it is an essential trace element and may therefore be less toxic to normal cells and thus lead to less harmful side effects.[10] The first copper-based AMN, a copper-phenanthroline complex was reported at the end of the 1970's;[11] since then, a great number of copper complexes were developed with interesting DNA-cleaving properties.[10, 12] Actually, two copper-based compounds (with 2,2'-bipyridine and 1,10-phenanthroline as N-donor ligands) from the Casiopeínas® family are currently in clinical trials.[13]

Some years ago, we have described three copper-terpyridine nitrato complexes with interesting cytotoxic properties.[14] In this previous study, the effect of supramolecular interactions on the biological properties was investigated, and the complex $[Cu(\mathbf{naphtpy})(NO_3)(H_2O)](NO_3)(MeOH)$ (where **naphtpy** stands for 4'-((naphthalen-2-yl)methoxy)-2,2′:6′,2″-terpyridine; Figure 1) exhibited notable cell toxicity behavior against several cancer cell lines.[14] In the present study, the ligand **naphtpy** was used to prepare copper(II) complexes with $CuCl_2$ and $Cu(ClO_4)_2$ as the metal sources (instead of $Cu(NO_3)_2$). For comparison purposes, copper complexes obtained by the reaction of 4′-chloro-2,2′:6′,2″-terpyridine (**Cltpy**; Figure 1) and $CuCl_2$ or $Cu(ClO_4)_2$ were synthesized as well. Hence, five copper compounds were obtained and characterized, and their interaction with DNA was subsequently examined. Lastly, their respective cytotoxicity against ovarian carcinoma cells (A2780), their cisplatin-resistant line (*i.e*. A2780cis) and human cervix adenocarcinoma cells (HeLa) was evaluated, which provided interesting data. Cell-cycle studies with HeLa cells were also carried out with the five complexes, comparing their behavior with that of cisplatin.

Results and Discussion

Preparation of the copper complexes

Reaction of **Naphtpy** with 1.5 equiv. of $CuCl_2{\cdot}2H_2O$ in methanol at 40 ºC produces the mixed-valence $Cu^{I}Cu^{II}$ compound

[a] J. Grau, Dr. A. Caubet, Dr. L. A. Barrios, Prof. P. Gamez
nanoBIC, Department of Inorganic and Organic Chemistry
Inorganic Chemistry Section, University of Barcelona
Martí i Franquès 1-11, 08028 Barcelona, Spain
E-mail: amparo.caubet@qi.ub.es
E-mail: patrick.gamez@qi.ub.es
[b] Dr. O. Roubeau
Instituto de Ciencia de Materiales de Aragón, CSIC and Universidad de Zaragoza, Plaza San Francisco s/n, 50009 Zaragoza, Spain
[c] Dr. J. Lorenzo
Institut de Biotecnologia i de Biomedicina and Departament de Bioquímica i de Biologia Molecular, Universitat Autònoma de Barcelona, Bellaterra, Barcelona, Spain
[d] Prof. P. Gamez
Catalan Institution for Research and Advanced Studies (ICREA)
Passeig Lluís Companys 23, 08010 Barcelona, Spain
[e] Prof. P. Gamez
Institute of Nanoscience and Nanotechnology (IN2UB)
Universitat de Barcelona, 08028 Barcelona, Spain

Supporting information for this article is given via a link at the end of the document.

$[Cu_3Cl_4(\mathbf{Naphtpy})_2][CuCl_2]$ (**1**). **1** crystallizes in the triclinic space group $P\bar{1}$ (see Table S1). Selected bond distances and angles are listed in Table S2.

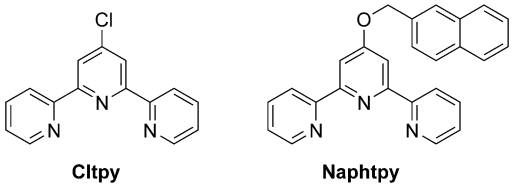

Figure 1. Representations of the ligands 4'-chloro-2,2':6',2''-terpyridine (**CItpy**) and 4'-((naphthalen-2-yl)methoxy)-2,2':6',2''-terpyridine(**Naphtpy**).

A representation of the solid-state structure of **1** is shown in Figure 2. The cationic part of **1**, namely $[\{CuCl(\mathbf{Naphtpy})\}_2(\mu\text{-}CuCl_2)]^+$, is formed by two square-pyramidal $[\{CuCl(\mathbf{Naphtpy})\}_2(\mu\text{-}CuCl_2)]^+$ units linked by a $[CuCl_2]^-$ unit. The anionic part of **1** is a linear $[Cl{-}Cu^I{-}Cl]^-$, which has been observed in structures described in the literature.[15] Hence, tetracopper compound **1** contains two copper(II) and two copper(I) ions. Since, the source of metal was copper(II) dichloride, the structure of **1** thus indicates that part of divalent copper was reduced during the synthesis. Actually, a number of copper-terpyridine complexes have been reported as catalysts for the oxidation of alcohols,[16] and even a mixed-valence Cu^ICu^{II} compound was described, which was obtained by partial reduction of copper(II) in the presence of TEMPO (*viz*. 2,2,6,6-tetramethylpiperidinyl-1-oxyl).[17] It can be pointed out here that this tendency of Cu/tpy complexes to undergo redox reactions is of great importance regarding their potential ability to oxidatively cleave DNA. In fact, it has been shown that copper-terpyridine complexes acting as good oxidation catalysts were also efficient DNA cleavers.[18] In the present case, it appears that the solvent of the reaction, namely methanol, is the reducing agent converting copper(II) into copper(I) ions. Thus, methanol is probably oxidised to methanal (and eventually to formic acid).

Reaction of **Naphtpy** with 1.5 equiv. of $Cu(ClO_4)_2{\cdot}6H_2O$ in methanol at 40 ºC yields the dinuclear compound $[Cu_2Cl_2(\mathbf{Naphtpy})_2](ClO_4)_2$ (**2**), whose crystal structure is depicted in Figure 2. As **1**, **2** crystallizes in the triclinic space group $P\bar{1}$ (see Table S1). Selected bond distances and angles are listed in Table S3. The solid-state structure of **2**, depicted in Figure 2, reveals that the dinuclear complex consists of a cationic $[\{CuCl(\mathbf{Naphtpy})\}_2(\mu\text{-}Cl)_2]^{2+}$ unit balanced by two perchlorate anions. The symmetry-related metal centres are in a square-pyramidal environment formed by a tridentate, N,N,N-**Naphtpy** ligand and a chloride in the square plane, a second chloride occupying the axial position (as observed for the copper(II) centres in **1**). The copper(II) ions are doubly bridged by chloride anions, and are separated by a distance of 3.5004(5) Å. The coordination bond distances and angles (see Table S3) are in normal ranges for such copper complexes.[19] Remarkably, **2** contains chloride ions whereas these anions were not added during the synthesis (see Experimental Section). Therefore, the chlorides are generated during the formation of **2**, most likely from the perchlorates. In effect, such chemical transformation of perchlorate to chloride has already been observed.[20]

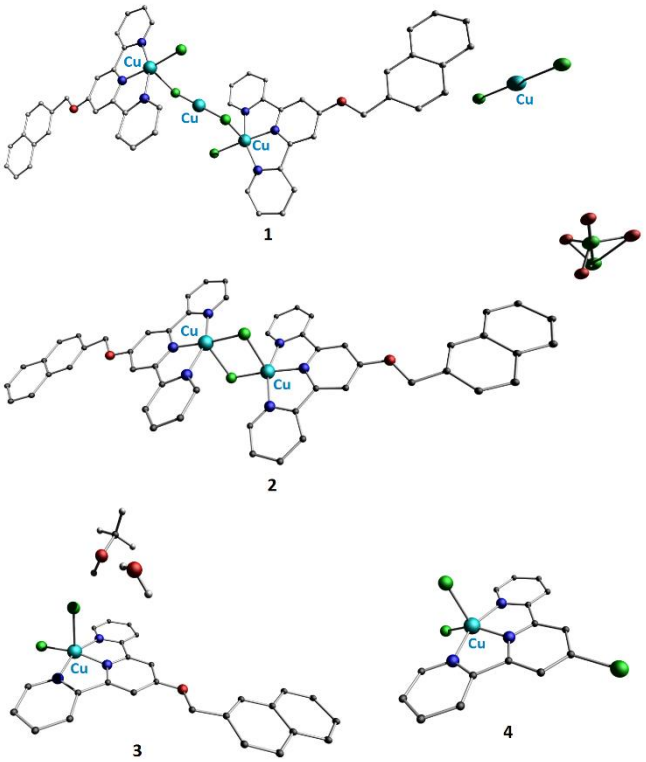

Figure 2. Representations of the molecular structures of $[Cu_3Cl_4(\mathbf{Naphtpy})_2][CuCl_2]$ (**1**), $[Cu_2Cl_2(\mathbf{Naphtpy})_2](ClO_4)_2$ (**2**), $[CuCl_2(\mathbf{Naphtpy})]_2(MeOH)_3(H_2O)$ (**3**) and $[CuCl_2(\mathbf{CItpy})]$ (**4**). H atoms (except for solvent molecules) are not shown for clarity.

It can be stressed here that ClO_4^- is commonly resistant to reduction although it is a strong oxidizing agent under acidic conditions, as evidenced by its relatively high standard potential (equation (1)):[21]

$$ClO_4^- + 8\,H^+ + 8\,e^- \leftrightarrow Cl^- + 4\,H_2O \qquad E_H^0 = 1.389\ V \qquad (1)$$

Thus, the fact that ClO_4^- was chemically transformed to Cl^- in the presence of Cu-**Naphtpy** species again illustrates their interesting redox properties (see compound **1** above), which can be important for their DNA-cleaving abilities. It can also be pointed out that perchlorate is an environmental contaminant;[22] Hence, such **Naphtpy**-containing copper complex may be applied to decontaminate ground water.

Reaction of **Naphtpy** with 1 equiv. of $CuCl_2{\cdot}2H_2O$ in methanol at 40 ºC produces the mononuclear compound $[CuCl_2(\mathbf{Naphtpy})]_2(MeOH)_3(H_2O)$ (**3**). **3** crystallizes in the monoclinic space group $P2_1/n$ (see Table S4). Selected bond distances and angles are listed in Table S5. The crystal structure of **3** is shown in Figure 2. The copper(II) ion is in a square-pyramidal environment formed by a terpyridine unit and a chloride anion in the basal plane, a second chloride anion

completing the coordination geometry at the axial position. The coordination bond distances and angles (see Table S5) are comparable with those reported in the literature for this compound.[23]

Reaction of **Cltpy** with 1 equiv. of $CuCl_2 \cdot 2H_2O$ in methanol at 40 ºC produces the mononuclear copper compound [$CuCl_2$(**Cltpy**)] (**4**), which crystallizes in the monoclinic space group $P2_1/c$ (Table S4). Selected bond distances and angles are listed in Table S6. The crystal structure of **4**, depicted in Figure 2, shows that the metal centre is in a square-pyramidal environment similar to that of compound **3** (see above and Figure 2). The coordination bond distances and angles (Table S6) are comparable with those observed for the structure already reported for this complex.[17]

Reaction of **Cltpy** with 1 equiv. of $Cu(ClO_4)_2 \cdot 6H_2O$ in methanol at 40 ºC yields the mononuclear copper compound [Cu(**Cltpy**)$_2$]$(ClO_4)_2$ (**5**); the crystal structure of **5** could not be determined but its elemental analysis suggests that it is the bis-**Cltpy** copper(II) complex depicted in Figure 3. Actually, the X-ray structure of this compound was reported.[24]

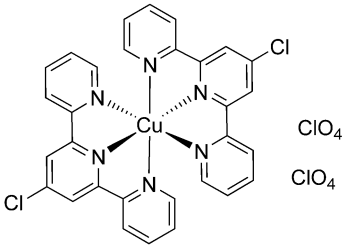

Figure 3. Proposed structure for compound **5**.

Interaction with DNA

The interaction of compounds **1**–**5** with DNA was subsequently investigated. First, gel electrophoretic studies were carried out with plasmid DNA. Structural changes induced by the interaction of the different copper complexes with the biomolecule can be visualized by the distinct electrophoretic mobilities of the consequent, various forms of DNA, namely Form I (supercoiled DNA), Form II (nicked DNA) and Form III (linear DNA). A reducing agent was used, namely ascorbic acid (1 mM), was used to simulate the reducing environment found in cells. A reference copper-based chemical nuclease, *i.e.* a bis-1,10-phenanthroline-copper species ([Cu(Phen)]$^{2+}$),[1] was used. The electrophoresis results achieved are shown in Figure 4.

Multinuclear compound **1** drastically affects the electrophoretic mobility of DNA. Indeed, at a concentration of 20 μM, Form I is converted into Form II (lane 6). Upon further increase of the concentration of **1**, the biomolecule is completely damaged (lanes 7–10). Dinuclear compound **2** appears not to be harmful to the double helix (Figure 4); at all complex concentrations (lanes 4–10), the bands corresponding to Form I and Form II are not modified in the presence of **2** (even at high concentrations), in contrast to the reference compound [Cu(Phen)]$^{2+}$ (lanes 2 and 3). Mononuclear compound **3** is more active than **2**, but much less damaging than **1**; some alteration of the DNA structure/conformation is only seen from a concentration of 80 μM (lanes 9 and 10).

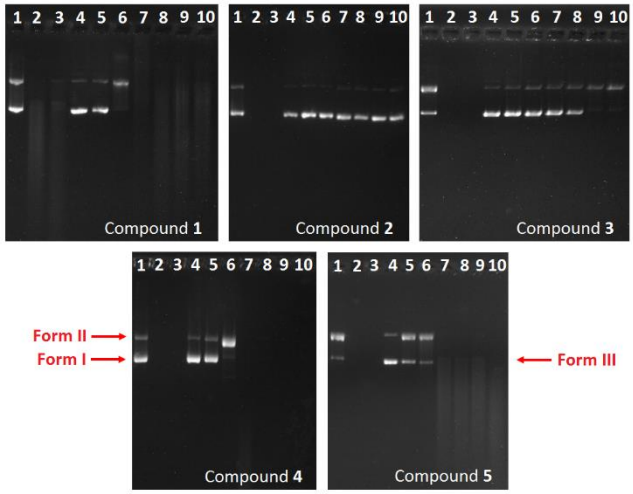

Figure 4. Agarose gel electrophoresis images of pBR322 plasmid DNA (15 μM b.p.) incubated for 1 h at 37 °C in cacodylate-NaCl buffer (pH 7.2) with increasing concentrations of compounds **1**–**5**, in the presence of a reducing agent, namely ascorbic acid (1 mM). For each compound (see corresponding image), lane 1: pure plasmid DNA; lane 2: [Cu(Phen)]$^{2+}$ = 5 μM (reference compound); lane 3: [Cu(Phen)]$^{2+}$= 100 μM; lane 4: [compound] = 5 μM; lane 5: [compound] = 10 μM; lane 6: [compound] = 20 μM; lane 7: [compound] = 40 μM; lane 8: [compound] = 60 μM; lane 9: [compound] = 80 μM; lane 10: [compound] = 100 μM.

Compound **4** is capable of efficiently cleaving DNA at a concentration of 20 μM, for which Form I is totally converted to mostly Form II and to some Form III (lane 6). At concentrations ≥ 40 μM, the DNA appears to be degraded into single-stranded pieces (lanes 7–10). Complex **5** is even more efficient since already a 10 μM solution of this compound produces a significant amount of Form II (lane 5). As for **4**, at concentrations ≥ 40 μM, **5** significantly damages the DNA (lanes 7–10).

In summary, the **Cltpy**-containing complexes **4** and **5** are comparatively more efficient DNA cleavers than the **Naphtpy**-based ones; only the mixed-valence complex **1** exhibits a similar cleaving activity to those of **4** and **5**. It can finally be pointed out that without ascorbic acid, the plasmid DNA is not affected (Figure S1); hence, the reducing agent is required to observe the (oxidative) cleaving activity of the complexes.

Competitive binding studies using intercalating ethidium bromide (EB) bound to *calf thymus* DNA (ct-DNA) were subsequently carried out. Hence, the potential displacement of EB by compounds **1**–**5** was followed by fluorescence spectroscopy (EB being strongly fluorescent when intercalated between DNA base pairs). Fluorescence spectra were thus recorded at constant concentrations of EB and ct-DNA, *viz*. 25 μM, by adding increasing quantities of the copper compounds; the range of concentrations used was 5–25 μM. The resulting quenching spectra for **1** are depicted in Figure 5, as a

representative example. The corresponding spectra for **2**–**5** are shown in Figure S2. It can be pointed out that all the complexes do not induce a significant release of EB, and that the **Naphtpy**-containing **1**–**3** are comparatively better fluorescence quenchers than **Cltpy**-containing **4** and **5**. This may be explained by the naphthyl group of the **Naphtpy** ligand, which may intercalate between base pairs and therefore expel some EB; actually, the same tendency was observed in a previous study with this family of ligands.[14]

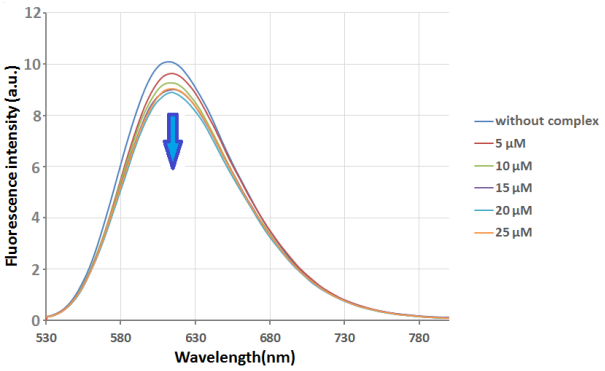

Figure 5. Emission spectra of the DNA-EB complex (25 µM), λ_{exc} = 514 nm, λ_{em} = 610 nm, upon addition of increasing amounts of complex **1** (5–25 µM). The blue arrow shows the diminution of the emission intensity with the increase in concentration of **1**.

The relative affinity of complexes **1–5** towards ct-DNA was evaluated by determining their Stern–Volmer constant K_{SV} applying equation (2), which allowed to compare their quenching efficiency.

$$\frac{I_0}{I} = 1 + K_{SV}[complex] \quad (2)$$

In equation (2), I_0 is the initial fluorescence intensity of EB bound to ct-DNA and I is the fluorescence intensity when adding increasing amounts of complex, in the range 5–25 µM. The K_{SV} constants achieved are listed in Table 1.

The K_{SV} values obtained are between 0.90 and 6.94 10^3 M^{-1}, well below the magnitude expected for classical intercalators, which is in the range 10^6 M^{-1} (*viz.* three orders of magnitude superior to that observed for **1**–**5**).[25] The K_{SV} values for **1**–**5** are in fact consistent with an external DNA-binding mode.[26] Such weak interactions with DNA were already suggested by the gel electrophoresis studies without reducing agent, which revealed that **1**–**5** were no able to significantly alter the structure/conformation of the double helix (see Figure S2).

Table 1. Stern–Volmer constants K_{SV} determined for **1–5** competing with DNA-bound EB[a]

Complex	K_{SV} (10^3 M^{-1})[b]	Log K_{SV}
1	6.94 ± 0.10	3.84
2	2.49 ± 0.32	3.40
3	5.96 ± 0.94	3.78
4	0.90 ± 0.13	2.95
5	1.21 ± 0.30	3.08

[a] K_{SV} is determined from the slope of the linear Stern–Volmer plot, i.e. I_0/I *versus* [complex], obtained using λ_{em} = 610 nm. [b] The results shown are means ± SD of at least three experiments.

The binding of compounds **1–5** to DNA was then investigated by UV-Vis spectroscopy.[27] Absorption spectra were recorded for 25 µM solutions of each complex to which were added increasing amounts of ct-DNA (from 1 to 25 µM). The corresponding spectra (range 190-400 nm) for **1**, which are representative for all the other compounds (*viz*. **2**–**5**), are shown in Figure S3.

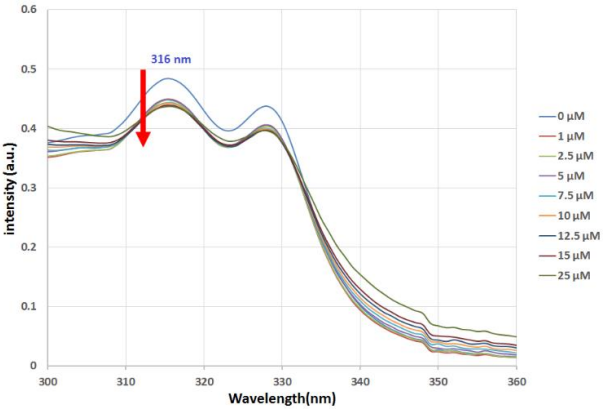

Figure 6. Absorption spectra (in the range 300-360 nm) of a 25 µM solution of **1** upon addition of increasing amounts of ct-DNA (1–25 µM). The MLCT band at λ = 316 nm was used to determine K_b. The red arrow shows the decrease in absorption intensity with increasing [ct-DNA].

Absorption bands in the range 300–360 nm, corresponding to metal-to-ligand charge transfer (MLCT), were used to examine the interaction of **1**–**5** with ct-DNA (Figures 6 and S4).

For **1**, a decrease of the absorption band at λ = 316 nm is observed when increasing the concentration of ct-DNA (Figure 6). No red shifts of the absorption bands take place, therefore indicating that **1** is not intercalating between base pairs,[28] as already suggested by the fluorescence studies (see above); in fact, it appears that **1** interacts electrostatically with the biomolecule.[29, 30] The intrinsic binding constant characterizing this interaction, namely K_b, can be estimated using equation (3):

$$\frac{[DNA]}{\varepsilon_a - \varepsilon_f} = \frac{[DNA]}{\varepsilon_0 - \varepsilon_f} + \frac{1}{K_b(\varepsilon_0 - \varepsilon_f)} \quad (3)$$

In equation (3), [DNA] represents the concentration of ct-DNA in base pairs, ε_a is the extinction coefficient at the given [ct-DNA], ε_f is the extinction coefficient of the free complex in solution (determined from A_{obs}/[complex]), and ε_0 is the extinction coefficient for the fully bound compound. The K_b values for **1**–**5** were thus determined, which are listed in Table 1.

Table 2. Intrinsic binding constants K_b determined for **1**–**5** interacting with ct-DNA[a]

Complex	K_b (10^6 M^{-1})[b]	Log K_b
1	3.41 ± 0.79	6.53
2	0.22 ± 0.06	5.34
3	1.05 ± 0.02	6.02
4	1.96 ± 0.64	6.29
5	0.71 ± 0.05	5.85

[a] The K_b values are determined from the ratio of the slope to the intercept of the corresponding linear [DNA]/($\varepsilon_a - \varepsilon_f$) *vs*. [DNA] plots, which are obtained for [complex] : [DNA] ratios ≤ 1:1 (λ = 316 nm (**1**), λ = 312 nm (**2**), λ = 315 nm (**3**), λ = 337 nm (**4**), λ = 322 nm (**5**)). [b] The results shown are means ± SD of at least three experiments.

A K_b value of 3.41 ± 0.79 10^6 M^{-1} is obtained for **1** (Table 1), illustrating a strong interaction of this compound with the double helix. Compounds **2**–**4** exhibit similar features (Figure S4 and Table 1), namely hypochromism without red shifting is observed, indicating that they are most likely acting as "outside binders".[30] Though, the interactions are weaker than that of **1**, with **1** >> **4** > **3** >> **2** (see Table 1).

Compound **5** shows a distinct behaviour; indeed, hyperchromism is observed (Figure S4). Both hypochromism and hyperchromism suggest structural changes of the DNA duplex. Hypochromism may be due to intercalation (if accompanied by a red shift) or to electrostatic contacts (as probably occurring with **1**–**4**) of the interacting compound.[31, 32] Hyperchromism may result from external binding (*e.g.* surface binding),[31, 33] for instance of a cationic species to the negatively charged phosphate backbone.[34] Thus, **5** appears to interact at the periphery of the DNA double helix.

Cytotoxicity assays

The cytotoxic properties of **1**–**5** were assessed using HeLa (cervix adenocarcinoma) cells, A2780 (ovarian carcinoma) cells and their cisplatin-resistant line A2780cis. IC_{50} values were determined after 24 and 72 hours of incubation at 37 °C. The data achieved for **1**–**5** and those reported for cisplatin are listed in Table 3.

The **Naphtpy**-containing complexes **1**–**3** exhibit good cytotoxic behaviours, with IC_{50} values in the submicromolar range after 72 h incubation (Table 3). Actually, **1**–**3** are 5 to 13 times more active than cisplatin against A2780 cells, and 17 to 46 more efficient than the platinum drug against A2780cis cells and even 42 to 180 times more active than cisplatin against HeLa cells. It can even be pointed out that **1** is slightly more cytotoxic towards the resistant A2780cis cells after 24 h incubation (4.44 *vs*. 6.09 µM; Table 3).

Table 3. IC_{50} values (µM)[a] for **1**–**5** and cisplatin against ovarian carcinoma (A2780) cells, their cisplatin-resistant line (A2780cis) and cervix adenocarcinoma (HeLa) cells, after 24 and 72 h of incubation.

	24 h		
Compd.	A2780	A2780cis	HeLa
1	6.09 ± 0.77	4.44 ± 0.66	7.12 ± 0.44
2	7.79 ± 1.04	9.27 ± 1.53	7.77 ± 1.32
3	10.4 ± 1.26	14.0 ± 2.66	14.04 ± 2.94
4	107 ± 13.2	128 ± 21.3	40.64 ± 23.75
5	44.1 ± 8.20	61.9 ± 17.18	29.24 ± 16.10
cisplatin	16.41[b]	74.97[b]	40.25 ± 3.71[d]
	72 h		
1	0.22 ± 0.02	0.30 ± 0.02	0.08 ± 0.02
2	0.27 ± 0.03	0.61 ± 0.07	0.13 ± 0.03
3	0.59 ± 0.05	0.79 ± 0.09	0.35 ± 0.14
4	0.90 ± 0.19	3.34 ± 0.80	1.44 ± 0.56
5	3.51 ± 1.43	3.62 ± 0.89	0.59 ± 0.15
cisplatin	2.8 ± 0.20[c]	13.8 ± 0.20[c]	14.66 ± 2.59[d]

[a] The IC_{50} (in µM) shown are mean values ± SE of three independent experiments. [b] IC_{50} values reported by Krieger et al.[35] [c] IC_{50} values reported by Raveendran et al.[36] [d] [b] IC_{50} values reported by Pilon et al.[37]

The activities of **CItpy**-based **4** and **5** are even more remarkable, particularly that of **4** (Table 3). In fact, while these compounds are poorly cytotoxic after 24 h incubation, they became significantly more efficient after 72 h incubation (Table 3). Hence, the activity of **5** is 13 times higher against A2780 cells after 72 h incubation, 17 times higher against A2780cis cells and 50 times against HeLa cells (Table 3). For **4**, the incubation-time effect is even more drastic; the cytotoxicity goes from 107 to 0.9 µM (ca. 120 times higher efficiency) with A2780 cells, and from 128 to 3.34 µM (38 times increased activity) with A2780cis ones and from 40.64 to 1.44 µM (28 times more active) against HeLa cells. Such variation of the cytotoxic properties of **4** (and of **5**) may be explained by a modification of the compound in solution with time. Therefore, absorption spectra of a solution of **4** were recorded during a period of 72 hours. The spectroscopic data

presented in Figure S5 only show the occurrence of a slight hyperchromism with time; no wavelength changes nor appearance of new bands are observed, thus suggesting that **4** is rather stable in solution. One possibility would be that the chlorine at the 4'-position of the ligand **Cltpy** is slowly hydrolysed, giving rise to the formation of more active (and more hydrophilic) species. However, more studies are definitely required to elucidate the exact origin of the "delayed" activities observed for **4** and **5**.

The resistant factors of A2780cis cells against cisplatin towards its parental cell line, range from 4.5 after 24 h to 5 after 72 h incubation time (Table S7). Complexes **1**–**5**, especially after 24 h incubation time, show little difference in cytotoxicity against A2780 cells and its resistant cell line, the resistant factors ranging from 0.7 to 1.4 (Table S7). After 72 h incubation time, the complexes also display reduced resistant factors in the A2780cis cell line towards the parental cell line, ranging from 1 to 3.7 (Table S7).

Apoptosis assays

Cells undergoing apoptosis specifically translocate phospholipids such as phosphatidylserine (PS) from the inner face of the plasma membrane to outside of the cell surface. Annexin-V is a phospholipid-binding protein having high affinity for phosphophatidylserine; therefore, detection of PS can be achieved by staining with Annexin-V followed by flow cytometry analysis. Cells are simultaneously stained with propidium iodide (PI), which can only enter cells with damaged plasma membrane and stains the DNA. Dual staining makes it possible to distinguish between early apoptotic cells (Annexin-V+, PI−) and late apoptotic (Annexin-V+, PI+) and necrotic/damaged cells (Annexin-V−, PI+). The results of Annexin-V/propidium iodide (PI) double staining study by flow cytometry are shown in Table 4. Viable cells are drastically reduced after 24 h of treatment at IC_{50} concentrations with cisplatin and copper complexes. Also, it was noticed that the rate of late apoptosis in HeLa cells treated with compound **4** was 14.68 %, a value close to that of cisplatin, whereas complexes **1**, **2**, **3** and **5** presented higher values from 21.5 to 29.5% (Table 4.). Finally, the ratio of early apoptotic cells decreased in all treatments with the copper compounds. It is also interesting to note that for compounds **1** and **2**, the percentage of cells in the R4 quadrant that corresponds to necrotic or damaged dead cells increased significantly from 7.94% in the case of cisplatin to 35.47 and 36.09% for **1** and **2**, respectively.

Table 4. Cell-cycle studies: percentages (%) of HeLa cells in each state after treatment with complexes **1**–**5** and cisplatin at IC_{50} concentrations for 24 h.

Compd.	vital cells (**R1**)	Early apoptotic cells (**R2**)	late apoptosis (**R3**)	necrotic/ damaged cells (**R4**)
Control	86.06	3.65	7.55	2.74
cisplatin	60.89	15.99	15.18	7.94
1	30.15	4.82	29.56	35.47
2	30.81	5.39	27.71	36.09
3	68.54	7.64	21.55	2.27
4	79.41	4.37	14.57	1.65
5	63.27	6.97	24.62	5.13

Conclusions

Five copper complexes have been prepared from terpyridine-based ligands with the objective to study their cytotoxic properties. The compounds all show interesting cytotoxic activities, but their cancer-cell growth inhibitory behaviors depend of the nature of the functional group at the 4' position of the terpyridine unit (*viz*. at the *para* position of the central pyridine ring). If this functional group is a naphthalen-2-yl group, *i.e.* compounds **1**–**3**, the activities observed are elevated after 24 h incubation with the three cell lines tested, clearly higher than that of cisplatin under the same experimental conditions. After 72 h incubation, IC_{50} values in the submicromolar range (down to 0.08 ± 0.02 µM (that is 80 nM) can even be achieved. Remarkably, when position 4' is occupied by a chlorine atom, the resulting copper complexes, namely compounds **4** and **5**, are almost inactive after 24 h incubation with the different cells, but their cytotoxic properties dramatically increase after 72 h of incubation. Hence, the IC_{50} values of **4** and **5** increase by up to 120 times, after 2 additional days of incubation. Such increase of the activity with time may be of interest for practical applications; it can indeed be interesting to administer a therapeutic compound whose activity is not immediate but is reached after some time (prodrug). These evolving behaviors of **4** and **5** may be explained by the slow hydrolysis of the 4'-chlorine (generating 4'-hydroxy-2,2':6',2''-terpyridine), producing species with improved cytotoxicity or/and hydrophilicity. This hypothesis will be verified in a subsequent study, whose results will be reported in due time.

Experimental Section

Materials: all reagents and solvents were obtained from commercial sources and used without further purification. $[Cu(H_2O)(1,10\text{-phenanthroline})_2](NO_3)_2$, the reference copper-based AMN, was prepared following a reported procedure.[38] The ligand 4'-((naphthalen-2-yl)methoxy)-2,2':6',2"-terpyridine (**Naphtpy**) was synthesized as described earlier.[14] pBR322 plasmid DNA was purchased from Roche and calf thymus DNA was obtained from Sigma-Aldrich.

Instrumentation and methods: All reactions were performed under aerobic conditions. ^{1}H and ^{13}C [39] NMR spectra were recorded at room temperature with a Varian Unity 400 MHz spectrometer. Proton and carbon chemical shifts are reported in parts per million (ppm, δ scale) and are referenced to the residual solvent peaks. Infrared spectra (KBr

pellets) were recorded in the range 4000–400 cm^{-1} using a Nicolet-5700 FT-IR, and data are represented as the frequency of absorption (cm^{-1}). UV-Vis experiments were done with a Varian Cary-100 spectrophotometer and the fluorescence measurements were performed with a KONTRON SFM 25 spectrofluorometer. Elemental analyses and ESI mass spectroscopy were performed by the Servei de Microanalisi, Serveis Cientificotècnics of the University of Barcelona. For the ESI MS, an LC/MSD-TOF Spectrometer from Agilent Technologies, equipped with an electrospray ionization (ESI) source was used.

Preparation of the copper(II) complexes

Compound 1: 0.195 mmol (76 mg) of **Naphtpy** was dissolved in 15 mL of warm methanol at 40 ºC. This solution was subsequently added to a warm methanolic solution (10 mL) of $CuCl_2{\cdot}2H_2O$ (0.293 mmol; 50 mg). The resulting reaction mixture was stirred at 40 ºC for 4 hours. After filtration, the blue solution obtained was left unperturbed for the slow evaporation of the solvent. Dark-green single crystals of **1**, suitable for X-ray diffraction measurements, were obtained with a yield of 71% (86 mg; based on **Naphtpy**). Elemental analyses calcd. for $C_{52}H_{38}Cl_6Cu_4N_6O_2$: C, 50.13; H, 3.07; N, 6.75. Found: C, 50.02; H, 3.25; N, 6.57. IR (KBr pellet): $\bar{\upsilon}$ = 3412, 3278, 3031, 2936, 1613, 1571, 1476, 1407, 1225, 1037, 1021, 822, 792 cm^{-1}.

Compound 2: 0.185 mmol (72 mg) of **Naphtpy** was dissolved in 15 mL of warm methanol at 40 ºC. Next, this solution was added to a warm methanolic solution of $Cu(ClO_4)_2{\cdot}6H_2O$ (0.270 mmol; 100 mg). The resulting reaction mixture was stirred at 40 ºC for 4 hours. After filtration, the blue solution obtained was left unperturbed for the slow evaporation of the solvent. Blue single crystals of **2**, suitable for X-ray diffraction measurements, were obtained with a yield of 79% (86 mg; based on **Naphtpy**). Elemental analyses calcd. for $C_{52}H_{42}Cl_4Cu_2N_6O_{12}$ (**2**–$2H_2O$): C, 53.12; H, 3.26; N, 7.15. Found: C, 54.74; H, 3.53; N, 7.62. IR (KBr pellet): $\bar{\upsilon}$ = 1613, 1556, 1480, 1356, 1087, 793, 618 cm^{-1}.

Compound 3: 0.439 mmol (171 mg) of **Naphtpy** was dissolved in 50 mL of warm methanol at 40 ºC. 0.440 mmol (75 mg) of $CuCl_2{\cdot}2H_2O$ was dissolved in 10 mL of methanol at 40 ºC. The two solutions were cooled down to room temperature and subsequently mixed. The resulting light-green solution was stirred at room temperature for 4 hours. After filtration, the solution was left unperturbed for the slow evaporation of the solvent. Blue single crystals of **3**, suitable for X-ray diffraction measurements, were obtained with a yield of 63% (160 mg; based on **Naphtpy**). Elemental analyses calcd. for $C_{52}H_{38}Cl_4Cu_2N_6O_2$ (**3**–3MeOH–H_2O): C, 59.61; H, 3.66; N, 8.02. Found: C, 60.41; H, 3.81; N, 8.27. IR (KBr pellet): $\bar{\upsilon}$ = 3417, 3057, 1604, 1570, 1478 cm^{-1}.

Compound 4: 0.385 mmol (103 mg) of **Cltpy** was dissolved in 15 mL of warm methanol at 40 ºC. This solution was subsequently added to a warm methanolic solution (10 mL) of $CuCl_2{\cdot}2H_2O$ (0.381 mmol; 65 mg). The resulting reaction mixture was stirred at 40 ºC for 4 hours. After filtration, the green solution was left unperturbed for the slow evaporation of the solvent. Light-green single crystals of **4**, suitable for X-ray diffraction measurements, were obtained with a yield of 83% (127 mg; based on Cu). Elemental analyses calcd. for $C_{15}H_{10}Cl_3CuN_3$: C, 44.80; H, 2.51; N, 10.45. Found: C, 44.80; H, 2.51; N, 10.45. IR (KBr pellet): $\bar{\upsilon}$ = 3091, 3034, 1591, 1557, 1470, 1417, 1017, 791 cm^{-1}.

Compound 5: 0.374 mmol (100 mg) of **Cltpy** was dissolved in 15 mL of warm methanol at 40 ºC. This solution was added to a warm solution of $Cu(ClO_4)_2{\cdot}6H_2O$ (0.351 mmol; 130 mg) in 10 mL of methanol. The resulting reaction mixture was stirred at 40 ºC for 4 hours. After filtration, the blue solution was left unperturbed for the slow evaporation of the solvent. **5** was obtained as a crystalline material with a yield of 42% (154 mg, based on copper). Elemental analyses calcd. for $C_{30}H_{20}Cl_6CuN_6O_8$, namely for $[Cu(\mathbf{Cltpy})_2](ClO_4)_2(H_2O)$: C, 44.16; H, 2.72; N, 10.30. Found: C, 44.62; H, 2.56; N, 10.10. IR (KBr pellet): $\bar{\upsilon}$ = 3357, 3080, 1597, 1558, 1476, 1247, 1086, 792, 622 cm^{-1}. It can be stressed that the solid-state structures of $[Cu(\mathbf{Cltpy})(ClO_4)_2(H_2O)]$[40] and $[Cu(\mathbf{Cltpy})_2](ClO_4)_2$[24] have been reported.

X-ray diffraction

Data for compounds **1**, **2**, 3 and **4** were obtained at 100 K on a Bruker APEX II CCD diffractometer at the Advanced Light Source beam-line 11.3.1 at Lawrence Berkeley National Laboratory, from a silicon 111 monochromator (λ = 0.77490 Å), respectively on a blue plate of dimensions 0.19 × 0.04 × 0.02 mm^3, a blue block of dimensions 0.04 × 0.03 × 0.01 mm^3, a blue-green block of dimensions 0.22 × 0.15 × 0.10 mm^3 and a blue-green block of dimensions 0.22 × 0.06 × 0.06 mm^3. Crystals of **1** were found to be twinned. Twinning was found within APEX using RLATT,[41] and then analysed with CELL_NOW[42] that found the proper unit cell, twinning law and ascribed reflection to either or both components. Cell refinement and integration were then performed by SAINT[41] as a 2-component twin, keeping the cell of both components identical. TWINABS[42] was used for absorption corrections and produced HKLF4 and HKLF5 data, respectively for initial structure solution and final refinement. Data reduction and absorption corrections for compounds **2**, **3** and **4** were performed with SAINT and SADABS,[43] respectively. The structures were solved by intrinsic phasing with SHELXT.[44] All structures were refined by full-matrix least-squares on F^2 with SHELXL.[45]

All details can be found in CCDC 1983582–1983585 that contain the supplementary crystallographic data for this paper. These data can be obtained free of charge from The Cambridge Crystallographic Data Center via https://summary.ccdc.cam.ac.uk/structure-summary-form. It should be noted that the structure of a polymorph of compound **4** has been reported (CCDC entry 1021666).[17]

Agarose Gel electrophoresis

Stock solutions of the different complexes were prepared in 1 mM sodium cacodylate–20 mM NaCl buffer (pH = 7.2). pBR322 plasmid DNA aliquots (0.01 mg mL^{-1}; 15 μM in base pairs) in 1 mM cacodylate–20 mM NaCl buffer were incubated with **1**–**4** for 1 h at 37 °C. For the studies with the presence of a reducing agent, ascorbic acid (1 mM cacodylate–20 mM NaCl buffer) was subsequently added (in the case of the experiments without ascorbic acid, this step was not done), and the resulting mixture was incubated at 37 °C for an additional hour. Then, the reaction samples were quenched with 4 μL of a xylene cyanol 1X aqueous solution (containing 30% (v/v) glycerol, 0.25% (w/v) bromophenol blue and 0.25% (w/v) xylene cyanol), and consequently electrophoretized in agarose gel (1% in TAE buffer) for 1 h at 1.5 V cm^{-1}, using a Bio-Rad horizontal tank connected to a Consort EV231 variable potential power supply. Afterwards, the DNA was stained with SYBR® safe and the gel was photographed with a BIORAD Gel Doc™ EZ Imager. Samples of free DNA and DNA in the presence of ascorbic acid were used as controls.

Fluorescence spectroscopy

Stock solutions (1 mL) of **1**–**4** (5 mM) were prepared in milli-Q water. These stock solutions were freshly prepared (*viz*. just before use). The samples to be analysed were prepared by addition of aliquots of the complex stock solutions (in the concentration range 5–200 μM.) to the appropriate volume of calf thymus DNA (ct-DNA) in 1 mM sodium

cacodylate–20 mM NaCl buffer (pH = 7.2). A solution ct-DNA/EB (*i.e.*, without complex) in cacodylate buffer was used as a blank. Fluorescence spectra were recorded at constant concentrations of EB and ct-DNA, namely 25 μM at room temperature, after 24 h incubation at 37 °C, on a Nandog™-Horiba Jobin Yvon spectrofluorometer with a 450 W xenon lamp using a computer for spectral subtraction and noise reduction. Each sample was scanned twice in a range of wavelengths between 500 and 730 nm, after excitation at 520 nm.

UV-Vis studies

Stock solutions (1 mL) of **1**–**4** (5 mM) were prepared in milli-Q water, just before use. The samples to be analysed were prepared by the addition of increasing amounts of ct-DNA (from 0 to 25 μM, in base pairs) to a 25 μM solution of the complex tested. The UV-Vis spectra were recorded using a Varian Cary-100 spectrophotometer.

Cytotoxicity studies

Human ovarian carcinoma cell line A2780 (ECACC 93112519) and its derived cisplatin-resistant cell line A2780 cis (ECACC 93112517) were routinely maintained in RPMI 1640 medium (Gibco) supplemented with 10% heat-inactivated Foetal Bovine Serum (FBS), GlutaMAX™ (Gibco) and 1% Antibiotic-Antimycotic solution (Gibco), in standard growth conditions (37 ºC and 5% CO_2). Human cervix adenocarcinoma cell line HeLa (ATCC CCL-2™) was routinely maintained in MEM α medium without nucleosides (Gibco) supplemented with 10% heat-inactivated FBS, GlutaMAX™ (Gibco) and 1% Antibiotic-Antimycotic solution (Gibco), in standard growth conditions. All tested compounds were kept in DMSO stocks at 50 mM and stored at -20 ºC. All working concentrations were prepared in cell culture media with a maximum of 0.5 % of DMSO.

Cells in exponential growth were plated in 96-well plates at a density of 3 × 10^3 cells/well and were allowed to grow overnight. Next, the cells were treated with different concentrations of each compound, ranging from 100 nM to 200 μM, during 24 h and 72 h of incubation, and 10 μL of PrestoBlue reagent (Invitrogen) were subsequently added following the standard protocol.[46] After 3 h of incubation, fluorescence was measured using a Victor3 multiwell microplate reader (excitation at 531 nm emission at 572 nm) (Perkin Elmer). The relative cell viability (%) for each sample related to the control cells without treatment was calculated. Each sample was tested in triplicates, in three independent experiments.

In vitro apoptosis assay

Induction of apoptosis *in vitro* by all compounds was determined by means of a flow cytometric assay with Annexin V-FITC by using an Annexin Annexin V-FITC Staining Kit (eBioscience, Thermo Scientific). HeLa cells in exponential growth were plated in 6-well plates at a density of 1 × 10^5 cells/well and were allowed to grow overnight. Subsequently, the cells were treated with each compound, using concentrations equal to their respective IC_{50} for 24 h (cisplatin was used as a reference, and untreated cells as a negative control). The cells were collected, washed with PBS, and resuspended in binding buffer (200 μL) and staining was accomplished by following the manufacturer's protocol. In brief, Annexin V–fluorescein isothiocyanate (FITC; 5 μL) and Propidium Iodide (10 μL) were added to the samples, which were then incubated 15 min at room temperature in the dark. The number of apoptotic cells was analysed by means of flow cytometry (FACSCalibur, Becton Dickinson).

Acknowledgements

Financial support from the Spanish Ministerio de Ciencia Innovación, y Universidades (Projects CTQ2017-88446-R AEI/FEDER, UE, RED2018-102471-T and RTI2018-098027-B-C22) is kindly acknowledged. P.G. acknowledges the Institució Catalana de Recerca i Estudis Avançats (ICREA).

Keywords: copper • oxidative cleavage • antineoplastic agents • cell death • chemical nuclease

[1] D. S. Sigman, A. Mazumder, D. M. Perrin, *Chem. Rev.* **1993**, *93*, 2295-2316.
[2] W. Yang, *Q. Rev. Biophys.* **2011**, *44*, 1-93.
[3] Z. Yu, J. A. Cowan, *Curr. Opin. Chem. Biol.* **2018**, *43*, 37-42.
[4] F. Mancin, P. Scrimin, P. Tecilla, U. Tonellato, *Chem. Commun.* **2005**, 2540-2548; F. Mancin, P. Scrimin, P. Tecilla, *Chem. Commun.* **2012**, *48*, 5545-5559.
[5] M. Diez-Castellnou, A. Martinez, F. Mancin, in *Advances in Physical Organic Chemistry, Vol 51, Vol. 51*, Academic Press Ltd-Elsevier Science Ltd, London, **2017**, pp. 129-186.
[6] R. F. Brissos, A. Caubet, P. Gamez, *Eur. J. Inorg. Chem.* **2015**, 2633-2645; G. Pratviel, in *Interplay between Metal Ions and Nucleic Acids, Vol. 10*, Springer, Dordrecht, **2012**, pp. 201-216.
[7] J. Y. Chen, J. Stubbe, *Nat. Rev. Cancer* **2005**, *5*, 102-112; W. Sneader, *Drug Discovery: A History*, John Wiley & Sons Ltd, Chichester, **2005**.
[8] R. M. Burger, K. Drlica, B. Birdsall, *J. Biol. Chem.* **1994**, *269*, 25978-25985; S. M. Hecht, *Bleomycin, Chemical, Biochemical, and Biological Aspects*, Springer-Verlag, New York, **1979**.
[9] C. M. Agbale, M. H. Cardoso, I. K. Galyuon, O. L. Franco, *Metallomics* **2016**, *8*, 1159-1169; J. C. Joyner, J. Reichfield, J. A. Cowan, *J. Am. Chem. Soc.* **2011**, *133*, 15613-15626.
[10] T. J. P. McGivern, S. Afsharpour, C. J. Marmion, *Inorg. Chim. Acta* **2018**, *472*, 12-39.
[11] D. S. Sigman, D. R. Graham, V. Daurora, A. M. Stern, *J. Biol. Chem.* **1979**, *254*, 2269-2272; K. A. Reich, L. E. Marshall, D. R. Graham, D. S. Sigman, *J. Am. Chem. Soc.* **1981**, *103*, 3582-3584.
[12] C. Wende, C. Ludtke, N. Kulak, *Eur. J. Inorg. Chem.* **2014**, 2597-2612.
[13] R. Galindo-Murillo, J. C. Garcia-Ramos, L. Ruiz-Azuara, T. E. Cheatham, F. Cortes-Guzman, *Nucleic Acids Res.* **2015**, *43*, 5364-5376; A. Vazquez-Aguirre, A. G. Gutierrez, R. M. Esparza, E. Hernandez-Lemus, L. Ruiz-Azuara, C. Mejia, *Anticancer Res.* **2019**, *39*, 3687-3695.
[14] J. Grau, R. F. Brissos, J. Salinas-Uber, A. B. Caballero, A. Caubet, O. Roubeau, L. Korrodi-Gregorio, R. Perez-Tomas, P. Gamez, *Dalton Trans.* **2015**, *44*, 16061-16072.
[15] H. Y. Liu, Z. T. Yu, Y. J. Yuan, T. Yu, Z. G. Zou, *Tetrahedron* **2010**, *66*, 9141-9144; Y. Cui, J. T. Chen, G. Chen, J. Ren, W. C. Yu, Y. T. Qian, *Acta Crystallogr. Sect. C-Cryst. Struct. Commun.* **2001**, *57*, 349-351.
[16] Z. Ma, L. J. Wei, E. Alegria, L. Martins, M. da Silva, A. J. L. Pombeiro, *Dalton Trans.* **2014**, *43*, 4048-4058; Y. R. Xi, W. Wei, Y. Q. Xu, X. Q. Huang, F. Z. Zhang, C. W. Hu, *Cryst. Growth Des.* **2015**, *15*, 2695-2702.
[17] G. Q. Zhang, E. Liu, C. X. Yang, L. Li, J. A. Golen, A. L. Rheingold, *Eur. J. Inorg. Chem.* **2015**, 939-947.
[18] K. Choroba, B. Machura, S. Kula, L. R. Raposo, A. R. Fernandes, R. Kruszynski, K. Erfurt, L. S. Shul'pina, Y. N. Kozlov, G. B. Shul'pin, *Dalton Trans.* **2019**, *48*, 12656-12673; K. Czerwinska, B. Machura, S. Kula, S. Krompiec, K. Erfurt, C. Roma-Rodrigues, A. R. Fernandes, L. S. Shul'pina, N. S. Ikonnikov, G. B. Shul'pin, *Dalton Trans.* **2017**, *46*, 9591-9604.
[19] J. Valdes-Martinez, D. Salazar-Mendoza, R. A. Toscano, *Acta Crystallogr. Sect. E.-Struct Rep. Online* **2002**, *58*, M712-M714.
[20] B. Bhattacharya, R. Dey, D. K. Maity, D. Ghoshal, *Crystengcomm* **2013**, *15*, 9457-9464.

[21] J. S. Cao, D. Elliott, W. X. Zhang, *J. Nanopart. Res.* **2005**, *7*, 499-506.
[22] T. Giblin, W. T. Frankenberger, *Microbiol. Res.* **2001**, *156*, 311-315.
[23] W. Henke, S. Kremer, D. Reinen, *Inorg. Chem.* **1983**, *22*, 2858-2863; E. J. Cho, S. Jung, K. Lee, H. J. Lee, K. C. Nam, H. J. Bae, *Chem. Commun.* **2010**, *46*, 6557-6559.
[24] W. Huang, W. You, L. Wang, C. Yao, *Inorg. Chim. Acta* **2009**, *362*, 2127-2135.
[25] Q. G. Chen, D. H. Li, Y. Zhao, H. H. Yang, Q. Z. Zhu, J. G. Xu, *Analyst* **1999**, *124*, 901-906.
[26] S. U. Rehman, Z. Yaseen, M. A. Husain, T. Sarwar, H. M. Ishqi, M. Tabish, *PLoS One* **2014**, *9*, 11.
[27] N. Shahabadi, P. Fatahi, *DNA Cell Biol.* **2012**, *31*, 1328-1334; R. F. Brissos, L. Korrodi-Gregório, R. Pérez-Tomás, O. Roubeau, P. Gamez, *Chem. Sq.* **2018**, *2*, 4.
[28] P. M. Bradley, A. M. Angeles-Boza, K. R. Dunbar, C. Turro, *Inorg. Chem.* **2004**, *43*, 2450-2452; J. K. Barton, A. T. Danishefsky, J. M. Goldberg, *J. Am. Chem. Soc.* **1984**, *106*, 2172-2176.
[29] S. Kashanian, S. Javanmardi, A. Chitsazan, K. Omidfar, M. Paknejad, *DNA Cell Biol.* **2012**, *31*, 1349-1355.
[30] M. I. Kwak, B. R. Jeon, S. K. Kim, Y. J. Jang, *ACS Omega* **2018**, *3*, 946-953.
[31] R. Tamilarasan, D. R. McMillin, *Inorg. Chem.* **1990**, *29*, 2798-2802.
[32] N. Sohrabi, N. Rasouli, M. Kamkar, *Bull. Korean Chem. Soc.* **2014**, *35*, 2523-2528.
[33] R. Vijayalakshmi, M. Kanthimathi, V. Subramanian, B. U. Nair, *Biochim. Biophys. Acta-Gen. Subj.* **2000**, *1475*, 157-162.
[34] Y. N. Xiao, C. X. Zhan, *J. Appl. Polym. Sci.* **2002**, *84*, 887-893.
[35] M. L. Krieger, N. Eckstein, V. Schneider, M. Koch, H. D. Royer, U. Jaehde, G. Bendas, *Int. J. Pharm.* **2010**, *389*, 10-17.
[36] R. Raveendran, J. P. Braude, E. Wexselblatt, V. Novohradsky, O. Stuchlikova, V. Brabec, V. Gandin, D. Gibson, *Chem. Sci.* **2016**, *7*, 2381-2391.
[37] A. Pilon, J. Lorenzo, S. Rodriguez-Calado, P. Adao, A. M. Martins, A. Valente, L. G. Alves, *ChemMedChem* **2019**, *14*, 770-778.
[38] K. J. Catalan, S. Jackson, J. D. Zubkowski, D. L. Perry, E. J. Valente, L. A. Feliu, A. Polanco, *Polyhedron* **1995**, *14*, 2165-2171.
[39] M. D. Youngblut, C. L. Tsai, I. C. Clark, H. K. Carlson, A. P. Maglaqui, P. S. Gau-Pan, S. A. Redford, A. Wong, J. A. Tainer, J. D. Coates, *J. Biol. Chem.* **2016**, *291*, 9190-9202.
[40] W. Huang, H. F. Qian, *J. Mol. Struct.* **2008**, *874*, 64-76.
[41] *SAINT and RLATT*, Bruker AXS Inc., Madison, Wisconsin, USA.
[42] G. M. Sheldrick, *CELL_NOW and TWINABS*, Bruker AXS Inc., Madison, Wisconsin, USA.
[43] L. Krause, R. Herbst-Irmer, G. M. Sheldrick, D. Stalke, *J. Appl. Crystallogr.* **2015**, *48*, 3-10.
[44] G. M. Sheldrick, *Acta Crystallogr. Sect. A* **2015**, *71*, 3-8.
[45] G. M. Sheldrick, *Acta Crystallogr. Sect. C-Struct. Chem.* **2015**, *71*, 3-8.
[46] M. L. Xu, D. J. McCanna, J. G. Sivak, *J. Pharmacol. Toxicol. Methods* **2015**, *71*, 1-7.

10.1002/cbic.202000154

WILEY-VCH

Entry for the Table of Contents

FULL PAPER

A series of copper-terpyridine complexes have been developed that exhibit delayed cytotoxicity and with the potential to induce apoptosis

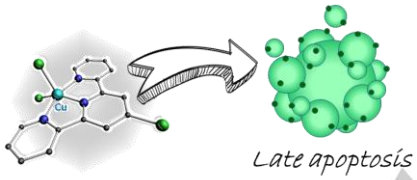

Jordi Grau, Amparo Caubet, Olivier Roubeau, David Monpeyó, Julia Lorenzo and Patrick Gamez**

Page No. – Page No.

Time-Dependent Cytotoxic Properties of Terpyridine-Based Copper Complexes